Journal of Manufacturing Processes 35 (2018) 672–680

Contents lists available at ScienceDirect

Journal of Manufacturing Processes

journal homepage: www.elsevier.com/locate/manpro

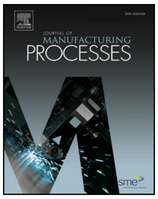

Technical Paper

On the printability and transformation behavior of nickel-titanium shape memory alloys fabricated using laser powder-bed fusion additive manufacturing

M. Mahmoudi[a], G. Tapia[a], B. Franco[b], J. Ma[b], R. Arroyave[b], I. Karaman[b], A. Elwany[a,*]

[a] *Department of Industrial & Systems Engineering, Texas A&M University, College Station, TX, United States*
[b] *Department of Materials Science & Engineering, Texas A&M University, College Station, TX, United States*

ARTICLE INFO

Keywords:
Additive manufacturing
Laser powder-bed fusion
Nickel-titanium
Transformation temperature
Printability
Shape memory alloys
Energy density
Delamination
Selective laser melting

ABSTRACT

Laser powder-bed fusion (L-PBF) additive manufacturing is regarded as an attractive alternative for producing parts with complex geometries for nickel-titanium shape memory alloys (NiTi SMAs). These alloys are known to pose challenges when processed using traditional subtractive or formative manufacturing technologies. Although L-PBF of NiTi has been investigated in some previous research efforts, very little emphasis has been placed on the manufacturability (or printability) of NiTi, where we use printability to refer to the capability of producing parts free of macroscopic defects.

The current study elucidates challenges related to the printability of NiTi SMAs using L-PBF, and its interaction with their phase transformation behavior, responsible for their functional properties. More specifically, we conduct experiments and employ machine learning classification techniques to identify an adequate design parameter and an empirical rule for determining the printability of NiTi. Our results indicate that the linear energy density E_L is a better design parameter for identifying satisfactory printability, while volumetric energy density, E_V, is more relevant in controlling the transformation behavior of the processed material.

1. Introduction

Since their discovery in the 1960s, nickel-titanium Shape Memory Alloys (NiTi SMAs) have found many applications in the automotive, aerospace, robotic, and biomedical industries [1]. SMAs are characterized by the shape memory effect (SME) and superelasticity (SE), which are the results of temperature-induced and deformation-induced reversible solid-to-solid phase transformations, respectively, enabling the part to recover its original shape after plastic deformation [2]. NiTi is a popular class of SMAs due to their biocompatibility [3], high transformation strain, high corrosion resistance, and high ductility [1]. Although NiTi SMAs have existed for approximately five decades and been used in various applications, the majority of manufactured NiTi parts have been limited to simple geometries such as wires, tubes, and sheets [4,5]. This is primarily because fabricating NiTi using conventional manufacturing methods such as machining, casting, or powder metallurgy and scaling up the production are difficult due to the high reactivity, and poor machinability of NiTi [6,7,3,8,9]. Furthermore, controlling the transformation behavior of NiTi SMAs is challenging due to their high sensitivity to compositional variations, which is exacerbated by the loss of Ti to the formation of oxides and carbides, and Ni evaporation during melting practices or fabrication using conventional powder metallurgy techniques. For example, less than 0.5 at. % composition change on the Ni side of the stoichiometry results in changes in transformation temperatures in excess of 100 °C [10,11].

The challenges noted above have inspired the investigation of new manufacturing technologies that can address some of these challenges. Metal Additive Manufacturing (AM) techniques have been proposed as viable candidates [3,4,12]. First, metal AM processes enable the production of NiTi parts with complex geometries due to the layerwise nature of the process. Moreover, modulating the manufacturing process parameters during metal AM can potentially be used to achieve control on composition and microstructure of processed NiTi, allowing for tailoring its functional response [13,14]. Among existing metal AM technologies, laser powder bed fusion (L-PBF) processes, commercially known as Selective Laser Melting (SLM) or Direct Metal Laser Sintering, is the most frequently investigated technique in the AM of NiTi due to its capability of producing parts with high feature resolution and

---

[*] Corresponding author.

E-mail addresses: mahmoudi@tamu.edu (M. Mahmoudi), gustavo@tamu.edu (G. Tapia), befranco@tamu.edu (B. Franco), jm@tamu.edu (J. Ma), rarroyave@tamu.edu (R. Arroyave), ikaraman@tamu.edu (I. Karaman), elwany@tamu.edu (A. Elwany).

https://doi.org/10.1016/j.jmapro.2018.08.037
Received 22 February 2018; Received in revised form 30 August 2018; Accepted 31 August 2018
1526-6125/

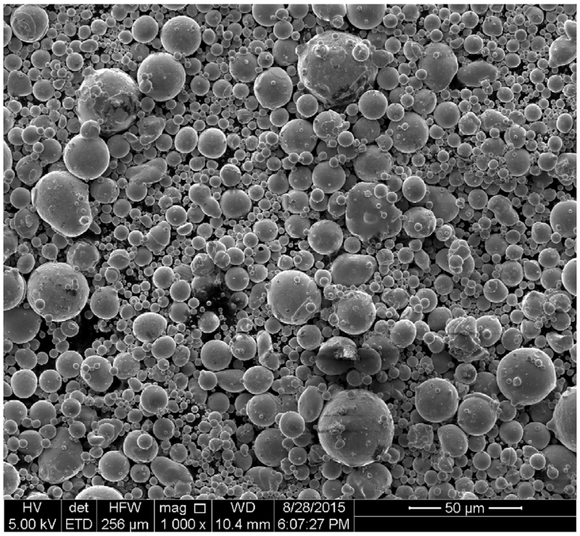

Fig. 1. SEM image of the initial NiTi powder of the process parameters used.

Table 1
Lower and upper bounds.

Parameter	P	v	h
Lowest level	35 W	70 mm/s	35 μm
Highest level	50 W	450 mm/s	120 μm

comparatively lower surface roughness than other AM processes like Directed Energy Deposition (DED). Due to the large number of process variables and parameters involved in L-PBF (e.g. laser power, scan speed, and hatch spacing) [15], successfully fabricating fully dense metal parts and controlling their properties require significant efforts in process planning and optimization, see for example [16–18]. Elahinia et al. has provided a recent review on the fabrication of NiTi alloys using AM, see [4].

The objective of the current study is to investigate the aspects related to the manufacturability of NiTi parts using L-PBF, and study the effect of different process parameters on the properties of these parts. More specifically, we investigate the effects of laser processing parameters (laser power, scan speed, and hatch spacing) on: (1) the ability of successfully producing macro defect-free parts, and (2) the transformation behavior of the fabricated parts. We discuss the effectiveness of previously proposed design parameters, such as volumetric energy density E_V, in planning successful fabrication of NiTi using manufacturing experiments, characterization techniques, and machine learning tools. Ultimately, we propose the linear energy density, E_L, as a more reliable design parameter for L-PBF of NiTi, and introduce a window of E_L within which NiTi parts are more likely to be successfully printed.

Prior works in the literature have studied various aspects related to the L-PBF of NiTi, including the effects of process parameters on structural and mechanical properties, density, impurity content, phase transformation, SME, and SE [12,19–24]. In most of these works, a maximum laser power of 100 W was employed, and energy density was defined as

$$\omega_V = \frac{P}{\rho_r \cdot d \cdot t \cdot v}, \tag{1}$$

Table 2
Experimental design matrix taking three process parameters into account as the variables.

Run No.	$P(W)$	$v(\mathrm{mm}/s)$	h (μm)	E_V (J/mm^3)	E_S (J/mm^2)	E_L (J/mm)	Building result
1	35.5	307	66	58.4	1.75	0.116	Defective
2	50	450	120	30.9	0.93	0.111	Defective
3	50	80	35	595.2	17.86	0.625	Non-defective
4	35	450	35	74.1	2.22	0.078	Defective
5	35	80	120	121.5	3.65	0.438	Defective
6	50	450	35	105.8	3.17	0.111	Defective
7	35	450	120	21.6	0.65	0.078	Defective
8	50	80	120	173.6	5.21	0.625	Non-defective
9	49.5	279	85	69.6	2.09	0.177	Defective
10	45.5	270	119	47.2	1.42	0.169	Defective
11	47.5	122	81	160.2	4.81	0.389	Defective
12	48	288	113	49.2	1.47	0.167	Defective
13	48.5	353	79	58.0	1.74	0.137	Defective
14	43.5	427	49	69.3	2.08	0.102	Defective
15	43	177	117	69.2	2.08	0.243	Defective
16	38	205	62	99.7	2.99	0.185	Defective
17	41	196	83	84.0	2.52	0.209	Defective
18	42.5	223	98	64.8	1.94	0.191	Defective
19	36.5	149	91	89.7	2.69	0.245	Defective
20	41	85	40	402.0	12.06	0.482	Non-defective
21	44	418	106	33.1	0.99	0.105	Defective
22	35	297	76	51.7	1.55	0.118	Defective
23	39	390	64	52.1	1.56	0.100	Defective
24	42	436	57	56.3	1.69	0.096	Defective
25	39.5	334	102	38.6	1.16	0.118	Defective
26	44	131	89	125.8	3.77	0.336	Defective
27	40	445	93	32.2	0.97	0.090	Defective
28	36.5	316	42	91.7	2.75	0.116	Defective
29	48.5	381	59	71.9	2.16	0.127	Defective
30	44.5	251	72	82.1	2.46	0.177	Defective
31	45	325	53	87.1	2.61	0.138	Defective
32	45.5	94	68	237.3	7.12	0.484	Non-defective
33	46	399	51	75.4	2.26	0.115	Defective
34	47	362	104	41.6	1.25	0.130	Defective
35	41.5	103	55	244.2	7.33	0.403	Defective
36	36	371	96	33.7	1.01	0.097	Defective
37	40.5	214	70	90.1	2.70	0.189	Defective
38	48.5	110	77	190.9	5.73	0.441	Defective
39	50	103	116	139.5	4.18	0.485	Defective
40	50	70	120	198.4	5.95	0.714	Non-defective
41	45.5	115	39	338.2	10.14	0.396	Defective
42	49	85	106	181.3	5.44	0.576	Non-defective
43	41	83	95	173.3	5.20	0.494	Defective
44	48	89	113	159.1	4.77	0.539	Non-defective
45	44.5	120	96	128.8	3.86	0.371	Defective
46	48.5	109	62	239.2	7.18	0.445	Non-defective
47	49	91	47	381.9	11.46	0.538	Non-defective

where P is the effective laser power (measured on the surface of the powder bed), ρ_r is the relative density of the powder bed, d is the laser beam diameter, t is the powder layer thickness, and v is the laser scan speed. To minimize variations in the phase transformation temperatures and minimize impurity content, an optimal set of process parameters was suggested with $P = 77$ W, $v = 200$ mm/s, $h = 50$ μm, corresponding to an energy density of $\omega_V = 234$ J/mm^3 [22]. In another study [25] by the same group, the volumetric energy density was introduced as

$$E_V = \frac{P}{h \cdot t \cdot v}, \tag{2}$$

where h is the laser hatch spacing; the distance between two adjacent passes of the laser beam within the same layer. It was shown that both austenitic and martensitic transformation temperatures for the fabricated parts are positively correlated with volumetric energy density since higher energy input results in: (1) preferential evaporation of